Light-Fuelled Self-Assembly of Cyclic Peptides into Supramolecular Tubules

Cissé, Nicolas; Kudernac, Tibor

Published in:
ChemSystemsChem

DOI:
10.1002/syst.202000012

Publication date:
2020

VIP *Very Important Paper*

Special Collection

Light-Fuelled Self-Assembly of Cyclic Peptides into Supramolecular Tubules

Nicolas Cissé[a, b] and Tibor Kudernac*[a, b]

The work performed by supramolecular polymers, such as microtubules and actin filaments, supports the life of the cell, and essentially involves fuel-driven self-assembly pathways. Developing fuel-driven supramolecular polymerization processes is therefore crucial to the realization of mechanically active molecular systems. Here, we demonstrate supramolecular tubules with non-equilibrium steady states that are fuelled by light. This dynamic supramolecular system features rapid cycles of self-assembly and disassembly, at rates that appear fast enough to perform mechanical tasks in fluids effectively.

Fluids are challenging environments for the work of molecules, being full of thermal noise, however nature has evolved strategies to produce useful mechanical work by harnessing molecular self-assembly. Typically, the chemically fuelled assembly of microtubules and actin filaments exerts sufficient force to displace micro-objects and deform supramolecular ensembles.[1] The mechanism by which the free energy of polymerization is converted into mechanical action is known as Brownian ratcheting.[2] Analogously, the self-assembly of any supramolecular polymer[3] could exert force. However, the strength of the force depends not only on the size of the building blocks and on the stiffness of the polymer,[2,4–6] but also on the rates of assembly and disassembly of the building blocks.[4] Hence, the central challenges towards the development of artificial microtubules include designing building blocks that can rapidly self-assemble into long and stiff supramolecular tubules and realizing transient and processive fuel-driven assembly.

While the growth of microtubules is realized by reversible conformational switching of building blocks fuelled by guanosine-triphosphate (GTP),[7] other chemical strategies can support the fuelling mechanism, as long as the fuel affects the supramolecular interactions between the building blocks. In examples of fuel-driven self-assembly reported so far, the role of the fuel is devised to modulate electrostatic interactions between the building blocks as to transiently switch between monomers and long supramolecular structures.[8–12] In all these cases the waste from the used fuel limits both the reversibility and processivity of the system. Here we report supramolecular tubules made of cyclic peptides whose transient growth is fuelled by light, through protonation by a photoacid.

The cyclic peptides are composed by an even number of alternating D- and L-amino acids.[13] The primary supramolecular interactions that allow self-assembly of cyclic peptides into tubules are the betasheet-type hydrogen bonding motives. In our design, we chose leucine as the only D- amino acid because leucine-rich cyclic peptides are known to form long and stiff supramolecular polymers,[14,15] through attractive hydrophobic interactions. Hydrogen-bonding and hydrophobic interactions are attractive interactions that can be counterbalanced by electrostatic repulsion to prevent the formation of aggregates. Typically, we have harnessed the charges carried by glutamic acid ($pK_a = 4.15$)[13] and histidine ($pK_a = 6.04$),[16,17] to design pH-responsive cyclic peptides.[15,18]

Specifically, the cyclic peptide (**CP**) on which we focus here contains three glutamic acid residues (Scheme 1). Further, a pyrene moiety was introduced because its aggregation-dependent fluorescence allows probing **CP** self-assembly.[19] A spiropyran-based photoacid was used to interfere with **CP** (Scheme 1). The open and protonated form of the photoacid, the merocyanine (**MEH**) switches to the closed spiropyran form (**SP**), and in so doing the photoacid releases protons that induce a significant pH change.[20,21] This reversible change can induce the assembly of inorganic nanoparticles or catalyse chemical reactions.[22,23]

As a building block, **CP** displays a hierarchical and pH-dependent self-assembly behaviour. Above pH = 6, the carboxylic acid residues at the periphery of the cyclic peptide ring are negatively charged (Figure 1). Individual **CP** rings repel each other thus effectively preventing the formation of any aggregates. Below pH = 5, the carboxylic acid residues protonate, thus promoting the formation of tubules, that further bundle into micro-fibres as evidenced by TEM and fluorescence microscopy (Figure 1a,b).

Detailed insight into the pH-dependence of the **CP** self-assembly behaviour is provided by fluorescence spectroscopy and zeta potential measurements (Figure 2, S1–S20). At higher pH values the monomeric form of **CP** yields intense emission bands with two maxima at $\lambda = 382$ nm and $\lambda = 400$ nm. The self-assembly of **CP** into (one-dimensional) tubules decreases the intensity of these bands. Further, an increase of an emission

[a] *N. Cissé, Dr. T. Kudernac*
MESA + Institute for Nanotechnology
University of Twente
Enschede, 7522 NB (The Netherlands)
E-mail: t.kudernac@rug.nl
[b] *N. Cissé, Dr. T. Kudernac*
Stratingh Institute for Chemistry
University of Groningen
4, 9747 AG, Groningen (The Netherlands)

Supporting information for this article is available on the WWW under https://doi.org/10.1002/syst.202000012

An invited contribution to a Special Collection on Fuelled Self-Assembly

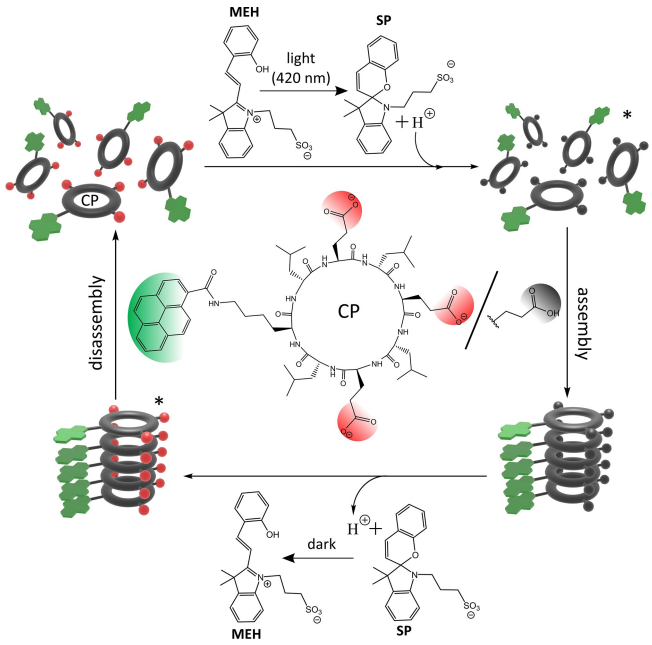

Scheme 1. Out-of-equilibrium assembly/disassembly cycling of cyclic peptide into tubules fuelled by a spiropyran photoswitch. The structures marked with asterisk (*) represent hypothetical transient out-of-equilibrium states reached upon full protonation/deprotonation of the **CP** building blocks. The actual assembly/disassembly processes is expected to occur before the building blocks are fully protonated/deprotonated.

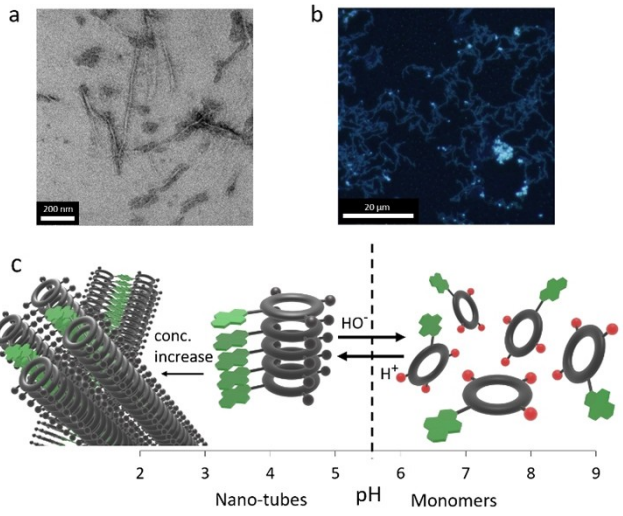

Figure 1. a) TEM image of a negatively stained sample of dried solution of **CP** at pH 3. b) Epifluorescence microscopy image of a dried solution of **CP** at pH 3. c) Schematic representation of the state of **CP** as a function of pH value.

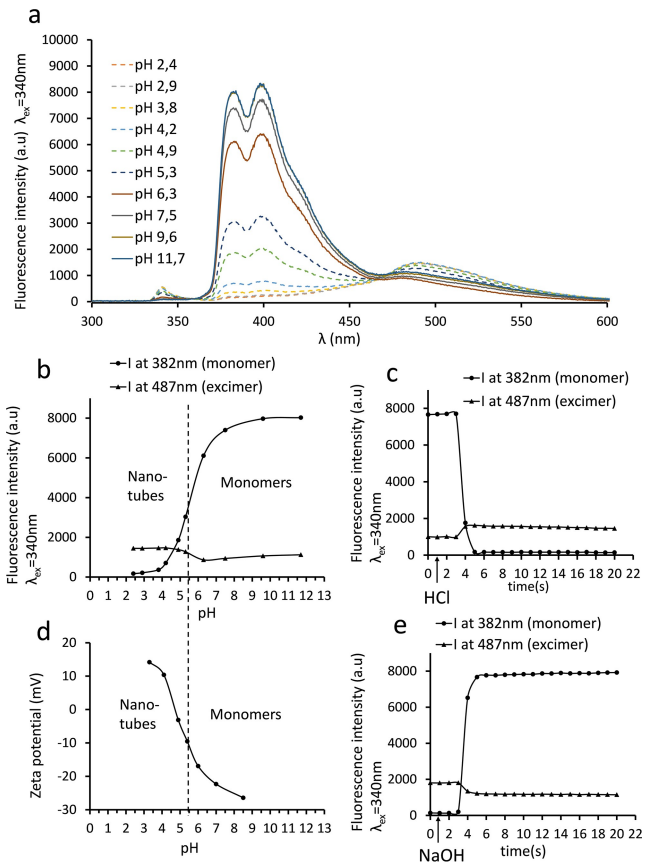

Figure 2. a) Fluorescence emission of CP (180 µM) at different pH values (λ_{ex} = 340 nm). b) Fluorescence emission of **CP** at λ = 382 nm and λ = 487 nm as a function of pH. c) Kinetics of assembly followed by changes of fluorescence emission intensity of **CP** (180 µM) at λ = 382 nm and λ = 487 nm as a function of time upon addition of HCl to adjust pH from 10 to 2. d) Zeta potential of **CP** (200 µM) as a function of pH. e) Disassembly as followed by changes in fluorescence emission intensity of **CP** (180 µM) at λ = 382 nm and λ = 487 nm, as a function of time upon addition of NaOH to adjust pH from 2 to 10.

at λ = 487 nm is observed as a consequence of excimer formation,[19] albeit only for **CP** concentrations above 0,2 mM (Figure S1–S8), when networks of thick bundles of tubules are formed (Figure S21). Conversely, thin and elongated, individual fibres are formed at **CP** concentrations below 0,2 mM (Figure S22–S24). The correlation between the morphology of the fibers and their fluorescence properties suggests that the tubules formed by **CP** are non-fluorescent pyrene complexes. The bundling of the tubules locally increases the pyrene density and allows excimer formation.[17]

A fast response to changes in pH is essential to evolve these cyclic peptides into future polymerization motors. When 10 µL of 0,2 M HCl are added to a stirred solution of **CP** (180 µM, 2,5 mL), the pH of the solution rapidly decreases from 10 to 2. This fast acidification triggers **CP** assembly into tubules in less than 4 seconds (Figure 2c). The assembly and disassembly kinetics of **CP** upon respective addition of acid and base were probed by fluorescence spectroscopy at different concentrations (Figure 2e, S9–S19).

Next, the photoacid was added to a **CP** solution, with the aim to fuel the assembly of **CP** in situ and reversibly. The concentration of the photoacid was kept to saturation (~8 mM), in order to maximize switching effects. The photoacid assumes the open protonated form **MEH** that absorbs light in the range that overlaps with the emission of pyrene (Figure S25a). As the concentration of **MEH** is a hundred times larger than the concentration of **CP**, any emission of **CP** is effectively filtered by

MEH. MEH switches to **SP** upon irradiation at $\lambda = 420$ nm and the photostationary state is constituted by at least 95% of **SP** (Figure S25a). **SP** is transparent in the range of pyrene emission, therefore simultaneous irradiation with $\lambda = 420$ nm and $\lambda = 340$ nm light maintains the photostationary state of **SP** and allows probing the extent of **CP** assembly, via pyrene emission. In these experiments, two light sources were placed on each side of a 1 cm large square cuvette and oriented perpendicularly to the detector. A pH-meter probe was immersed in the top part of the cuvette and the solution was stirred at 2000 r.p.m. Under these conditions, the final state of the **CP** and **SP** mixture displays similar pH-dependent assembly behaviour as **CP** alone: monomeric **CP** dominates at pH > 5.5, whereas the majority of **CP** is assembled at a lower pH (Figure 3).

The capacity of the photoacid to alternate the pH of the solution in the presence of **CP** was verified for different concentrations of **CP**; carboxylic acid residues of **CP** buffer the overall measured pH change, hence larger **CP** concentrations result in pH oscillations of smaller amplitude (Figure S25b).

The pH oscillates between 6,1 and 4,9 when the mixture of **CP** (73 μM) and **SP** (8.3 mM) is irradiated at $\lambda = 340$ nm, and $\lambda = 420$ nm for 90 s followed by 180 s dark relaxation (Figure 4a). The emission intensity of the monomeric state was followed in time in order to estimate the extent of **CP** assembly (Figure 4c). Interpretation of the curves also considers that **CP** emission is filtered by **MEH**. pH measurements directly translate to the progress of **MEH** conversion into **SP** and indicate that the photostationary state is reached after 25 s of irradiation (Figure 4b). The initial increase in fluorescence intensity corresponds to this photo-conversion process (Figure 4c). Once photostationary state is reached, the emission of the monomeric state can be compared to the calibration curve (Figure 3b); and the decrease in emission intensity of monomeric **CP** is a consequence of the assembly process (Figure 4c). After ~ 100 s of irradiation, the fluorescence intensity stabilizes once approximately 82% of **CP** is assembled into tubules (Figure 4c, Figure 3b). During the relaxation in the dark, as the disassembly kinetic is fast (Figure 2c), the specific pH value provides an accurate estimation of the extent of **CP** assembly by comparison to the calibration curve (Figure 3b). The pH levels off at pH = 6.1, after 200 s in the dark, which corresponds to approximately 90% of **CP** molecules being in the monomeric state.

Notably, the assembly of CP is slower during the first irradiation cycle despite the fact that the pH value decreases at the same rate during each irradiation (Figure 4b,4c). During the first irradiation, approximately 72% of **CP** is assembled once

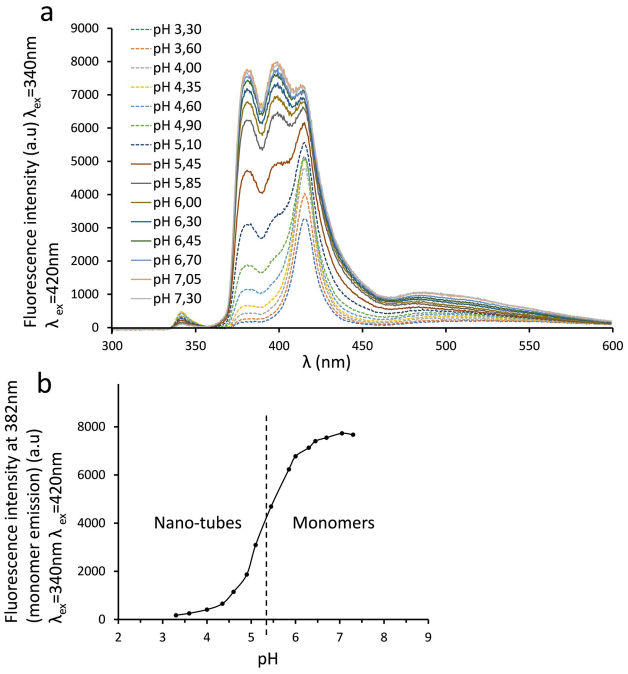

Figure 3. a) Fluorescence emission of the mixture of **CP** (73 μM) and **SP** (8.3 mM) at different pH values acquired after 90 s dual irradiation with $\lambda_{ex} = 340$ nm and $\lambda_{ex} = 420$ nm light. b) Fluorescence emission intensity of the mixture of **CP** (73 μM) and **SP** (8.3 mM) at 382 nm (monomer emission) as a function of pH. Samples are irradiated for 90 s simultaneously at $\lambda_{ex} = 340$ nm and 420 nm.

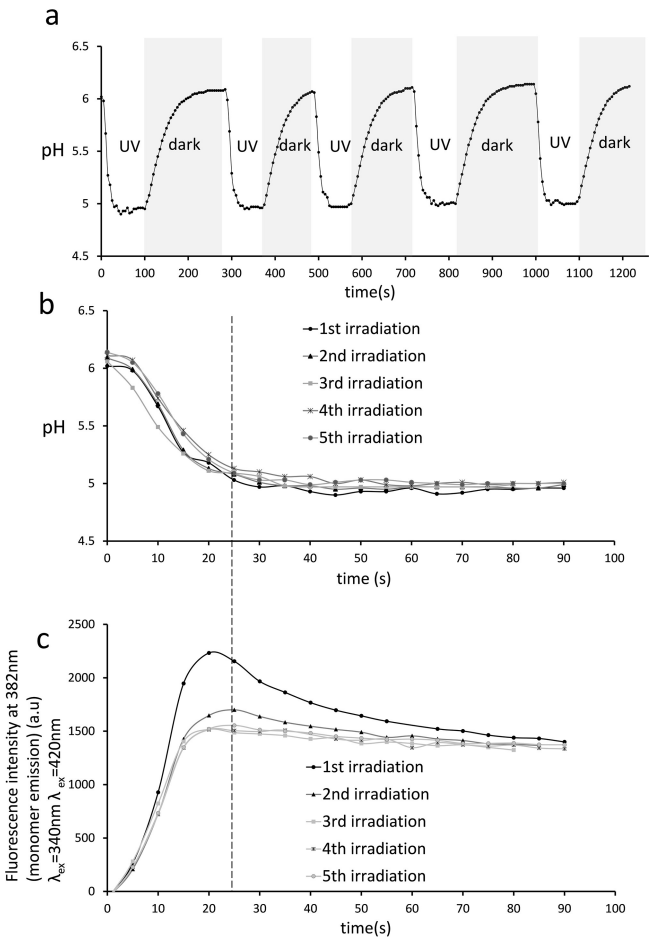

Figure 4. a) pH oscillations of the mixture of **CP** (73 μM) and **SP** (8.3 mM) in water upon dual irradiation ($\lambda_{ex} = 340$ nm and $\lambda_{ex} = 420$ nm) cycles. b) pH value of the **CP** (73 μM) and **SP** (8.3 mM) mixture during the dual irradiation. c) Fluorescence emission intensity at 382 nm (monomer emission) of the mixture of **CP** (73 μM) and **SP** (8.3 mM) during consecutive dual irradiations ($\lambda_{ex} = 340$ nm + 420 nm).

photostationary state is reached, whereas during subsequent irradiations, **CP** is already fully assembled (approximately 82%) once photostationary state is reached. Presumably, faster assembly in subsequent irradiation cycles is caused by the presence of tubular fragments that remain after 200 s of relaxation in the dark. These fragments act as nuclei for tubular growth.

The intensity of light allows controlling the rate of **MEH** conversion into **SP**. Different intensities were used to reach the photostationary state in 90, 25 and 15 seconds, respectively (Figure 5, S26–S31). Although **CP** emission is filtered before the photostationary state is reached, most of **CP** self-assembly does happen steadily with the decrease of the pH following the **MEH** photo-conversion to **SP**. We conclude that the rate and extend of **CP** assembly is affected by light intensity, which means that a wide range of fuelled states can be potentially reached.

After drop-casting and drying under illumination, long and thin fibres are visible on electron microscopy micrographs (Figure 6a). These fibres correspond to bundles of individual tubules surrounded by an amorphous mass that is likely constituted by photoacid. In contrast, samples that were drop casted and dried in the dark both before any irradiation (Figure S32) or after irradiation followed by dark relaxation (Figure 6b, S33), reveals undeveloped fibres. These small fragments of tubules correspond to the small fraction of **CP** (~10%) being in the assembled state for the given pH as evaluated from the calibration curve (Figures 3b and 4).

In summary, we demonstrate a system in which light fuels cycles of fast supramolecular polymerization and depolymerization through the control of the charged state of the monomer. Using light as a fuel allows achieving spatio-temporal control over the delivery of the fuel to the system, while producing no waste products. Such a system has potential to operate continuously and repeatedly, without the need to exchange material with the external environment. Moreover, light intensity can be used as a control to tune association and dissociation rates as well as to access any given self-assembled state. Overall, this supramolecular system demonstrates a dynamic behaviour that is key to the operation of artificial polymerization machines capable of performing useful tasks in fluids.

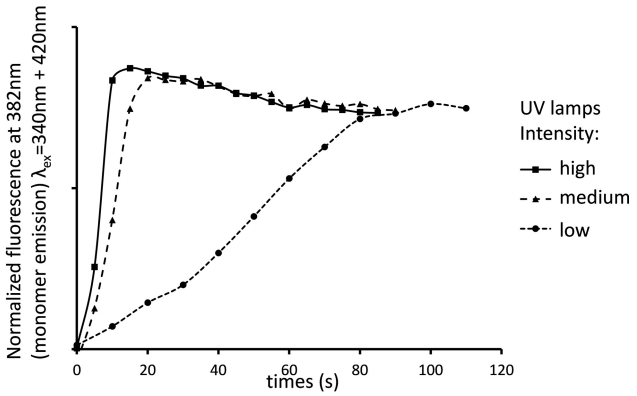

Figure 5. Normalized fluorescence emission intensity at $\lambda = 382$ nm (monomer emission) of the mixture of **CP** (73 μM) and **SP** (8.3 mM) during the fourth dual irradiation cycle ($\lambda_{ex} = 340$ nm + 420 nm).

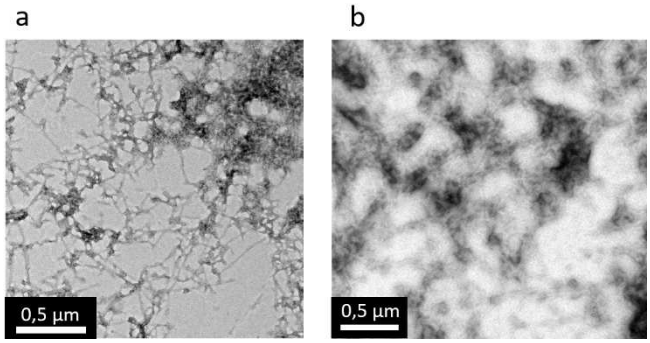

Figure 6. a) TEM micrograph of negatively stained samples of the mixture of **CP** and **SP**([**CP**] = 73 μM and [**SP**] = 8.3 mM) dried under continuous UV irradiation after 5 irradiation cycles, pH = 6.1. b) TEM micrograph of the mixture of **CP** and **SP** dried in the dark after 5 irradiation cycles, pH = 6.1.

Experimental Section

Experimental details on the synthesis and characterization of the building blocks (Scheme S1, Figure S34–S35), the fluorescence spectroscopy, and the electron microscopy can be found in the supporting information.

Acknowledgements

N.C. is supported by the curiosity-driven research program ECHO (712.017.002) which is financed by the Dutch Research Council (NWO). T.K. thanks the ERC (Consolidator Grant, MechanoTubes, 819075) for funding. Romain Chevallier-Senyk is acknowledged for assistance with synthesis and Dr. Rico Keim is acknowledged for assistance with TEM.

Conflict of Interest

The authors declare no conflict of interest.

Keywords: artificial microtubules · cyclic peptides · fuelled self-assembly · molecular switches · supramolecular polymers

[1] M. Vleugel, M. Kok, M. Dogterom, *Cell Adhes. Migr.* **2016**, *10*, 475–494.
[2] G. Oster, *Nature* **2002**, *417*, 25.
[3] E. Krieg, M. M. C. Bastings, P. Besenius, B. Rybtchinski, *Chem. Rev.* **2016**, *116*, 2414–2477.
[4] R. D. Astumian, *Science* **1997**, *276*, 917–922.
[5] J. A. Theriot, *Traffic* **2000**, *1*, 19–28.
[6] J. W. Fredy, A. Méndez-Ardoy, S. Kwangmettatam, D. Bochicchio, B. Matt, M. C. A. Stuart, J. Huskens, N. Katsonis, G. M. Pavan, T. Kudernac, *Proc. Mont. Acad. Sci.* **2017**, *114*, 11850–11855.
[7] T. Mitchison, M. Kirschner, *Nature* **1984**, *312*, 237–242.
[8] J. Boekhoven, W. E. Hendriksen, G. J. M. Koper, R. Eelkema, J. H. van Esch, *Science* **2015**, *349*, 1075–1079.
[9] J. Boekhoven, A. M. Brizard, K. N. K. Kowlgi, G. J. M. Koper, R. Eelkema, J. H. van Esch, *Angew. Chem. Int. Ed.* **2010**, *49*, 4825–4828.

[10] J. Leira-Iglesias, A. Sorrenti, A. Sato, P. A. Dunne, T. M. Hermans, *Chem. Commun.* **2016**, *52*, 9009–9012.
[11] S. Maiti, I. Fortunati, C. Ferrante, P. Scrimin, L. J. Prins, *Nat. Chem.* **2016**, *8*, 725–731.
[12] B. G. P. van Ravensteijn, W. E. Hendriksen, R. Eelkema, J. H. van Esch, W. K. Kegel, *J. Am. Chem. Soc.* **2017**, *139*, 9763–9766.
[13] M. R. Ghadiri, J. R. Granja, R. A. Milligan, D. E. McRee, N. Khazanovich, *Nature* **1993**, *366*, 324.
[14] D. J. Rubin, S. Amini, F. Zhou, H. Su, A. Miserez, N. S. Joshi, *ACS Nano* **2015**, *9*, 3360–3368.
[15] H. Shaikh, J. Y. Rho, L. J. Macdougall, P. Gurnani, A. M. Lunn, J. Yang, S. Huband, E. D. H. Mansfield, R. Peltier, S. Perrier, *Chem. Eur. J.* **2018**, *24*, 19066–19074.
[16] A. Méndez-Ardoy, J. R. Granja, J. Montenegro, *Nanoscale Horiz.* **2018**, *3*, 391–396.
[17] A. Mendez-Ardoy, A. Bayón-Fernández, Z. Yu, C. Abell, J. R. Granja, J. Montenegro, *Angew. Chem. Int. Ed.* n.d., *n/a*, DOI 10.1002/anie.202000103.
[18] S. M. Darnall, C. Li, M. Dunbar, M. A. Alsina, S. Keten, B. A. Helms, T. Xu, *J. Am. Chem. Soc.* **2019**, DOI 10.1021/jacs.9b03732.
[19] G. K. Bains, S. H. Kim, E. J. Sorin, V. Narayanaswami, *Biochemistry* **2012**, *51*, 6207–6219.
[20] R. Klajn, *Chem. Soc. Rev.* **2014**, *43*, 148–184.
[21] L. Kortekaas, W. R. Browne, *Chem. Soc. Rev.* **2019**, *48*, 3406–3424.
[22] D. Samanta, R. Klajn, *Adv. Opt. Mater.* **2016**, *4*, 1373–1377.
[23] C. Maity, W. E. Hendriksen, J. H. van Esch, R. Eelkema, *Angew. Chem. Int. Ed.* **2015**, *54*, 998–1001.

Manuscript received: February 20, 2020
Version of record online: May 4, 2020

